The Antarctic Mantle: a Petrological, Geophysical, Geodynamic, and Geodetic View

7. Mantle Convection and Surface Manifestations

7.1. Mantle Convection and Plumes

Eva Bredow[1] and Bernhard Steinberger[2,3]

[1] *Department of Geosciences, Kiel University, Kiel, Germany.*

[2] *GFZ German Research Centre for Geosciences, Potsdam, Germany.*

[3] *Centre for Earth Evolution and Dynamics, University of Oslo, Oslo, Norway.*

E-mail: eva.bredow@ifg.uni-kiel.de, bstein@gfz-potsdam.de

Mantle Convection and Possible Mantle Plumes beneath Antarctica – Insights from Geodynamic Models and Implications for Topography

Abstract

This chapter describes the large-scale mantle flow structures beneath Antarctica as derived from global seismic tomography models of the present-day state. In combination with plate reconstructions, the time-dependent pattern of paleosubduction can be simulated and is also shown from the rarely seen Antarctic perspective. Furthermore, a dynamic topography model demonstrates which kind and scales of surface manifestations can be expected as a direct and observable result of mantle convection. The last section of the chapter features an overview of the classical concept of deep-mantle plumes from a geodynamic point of view and how recent insights, mostly from seismic tomography, have changed the understanding of plume structures and dynamics over the past decades. The long-standing and controversial hypothesis of a mantle plume beneath West Antarctica is summarised and addressed with geodynamic models, which estimate the excess heat

flow of a potential plume at the bedrock surface. However, the predicted heatflow is small while differences in surface heat flux estimates are large, therefore the results are not conclusive with regard to the existence of a West Antarctic mantle plume. Finally, it is shown that global mantle flow would cause tilting of whole-mantle plume conduits beneath West Antarctica such that their base is predicted to be displaced about 20° northward relative to the surface position, closer to the southern margin of the Pacific Large Low Shear Velocity Province.

7.1.1 Large-Scale Mantle Flow Beneath Antarctica

Mantle convection is the main mode how heat, both from the Earth's initial formation and continuously re-generated through radioactive decay, is transported from the deep Earth interior to near its surface (Schubert et al. 2001). Increase in temperature would lead to a reduction of viscosity, and it is standard theory that through a negative feedback the Earth will maintain a temperature such that it is sufficiently "soft" to convect and loose its heat in that way (Tozer 1972). However, such self-regulation might be prevented due to the effect of mantle melting on viscosity (Korenaga 2016). Since the Earth's heat flux is not balanced by radiogenic heat production, the Earth is cooling with time (Korenaga 2008). Primary evidence is the greater prevalence of komatiites in the Archean, but radiogenic heating will be better constrained by future measurements of geoneutrino flux. The rheology of mantle materials is very poorly known; even for radial mantle viscosity structure, a wide variety of models has been proposed in recent years (e.g. Steinberger & Calderwood 2006; Čížková et al. 2012; Justo et al. 2015; Marquardt & Miyagi 2015; Roy & Peltier 2015; Rudolph et al. 2015; King 2016; Lau et al. 2016; Liu & Zhong 2016; Nakada et al. 2017). Hence there are large uncertainties in the mantle flow structure. However, there are certain observables that can be obtained as model output from mantle flow computations and compared to observed values; in this way, flow structure can be better constrained. Especially the large-scale geoid can be predicted quite successfully (Hager & Richards 1989), and therefore there is some confidence into models of at least the large-scale flow structure.

The tectonic plates are the surface expression of mantle convection. In particular, where plates converge, in most cases one of them will dive into the mantle, as it is cold and heavy, and the sinking plates are essential drivers of plate tectonics (Forsyth & Uyeda 1975) and mantle convection (Davies 1977; Conrad & Lithgow-Bertelloni 2002). One way of reconstructing mantle structure and flow is hence based on plate reconstructions – where plates have been converging and sinking throughout geologic history (Richards & Engebretson 1992; Ricard et al. 1993; Bunge et al. 2002; Shephard et al. 2012). Another main source of information on mantle structure is seismic tomography (e.g. Dziewonski & Woodhouse 1987; Becker & Boschi 2002; Grand 2002; Montelli et al. 2006; Schaeffer & Lebedev 2013; French & Romanowicz 2015; Hosseini et al. 2019): regions with fast seismic velocity anomalies are thought to be colder, denser and hence likely sinking, whereas regions with slow anomalies are hotter, less dense and buoyantly rising. If seismic anomalies are largely due to temperature variations, the latter can be computed based on mineral physics (Steinberger & Calderwood 2006; Fullea et al. 2009). Ideally, the mantle temperature and density structure inferred from tomography should closely match that inferred from subduction history. In practice, there is at least some similarity between them on the largest scales (Shephard et al. 2012; Steinberger et al. 2012).

On these largest scales, one feature that probably has been present for the last 300 Myr or so is the "Ring of Fire" – a ring of subduction zones surrounding the basin of the Pacific, and its predecessor, the Panthalassic Ocean (Figure 1)(Steinberger et al. 2012; Domeier & Torsvik 2019). As slabs in this circum-Pacific belt mostly cause sinking flow, there must be rising flow elsewhere. Hence, there are probably also two antipodal regions of rising flow, one beneath the Pacific and one beneath Africa, and mantle flow is dominated by a large-scale spherical harmonic degree-two (or quadrupolar) structure (Conrad et al. 2013). These regions of rising mantle flow roughly overlay the two Large Low Shear Velocity Provinces (LLSVPs) of the lowermost mantle. Figure 1 shows, from a south polar perspective, how this ring of subduction zones has been continous roughly across the present-day location of Antarctica until around 80 Myr ago. Since then, southward subduction of the Phoenix plate (which has now completely disappeared) has mostly stopped. Subduction continues on either side of it – north of New Zealand and beneath South America. But given that slabs probably take 200 to 300 Myr to sink to the base of the

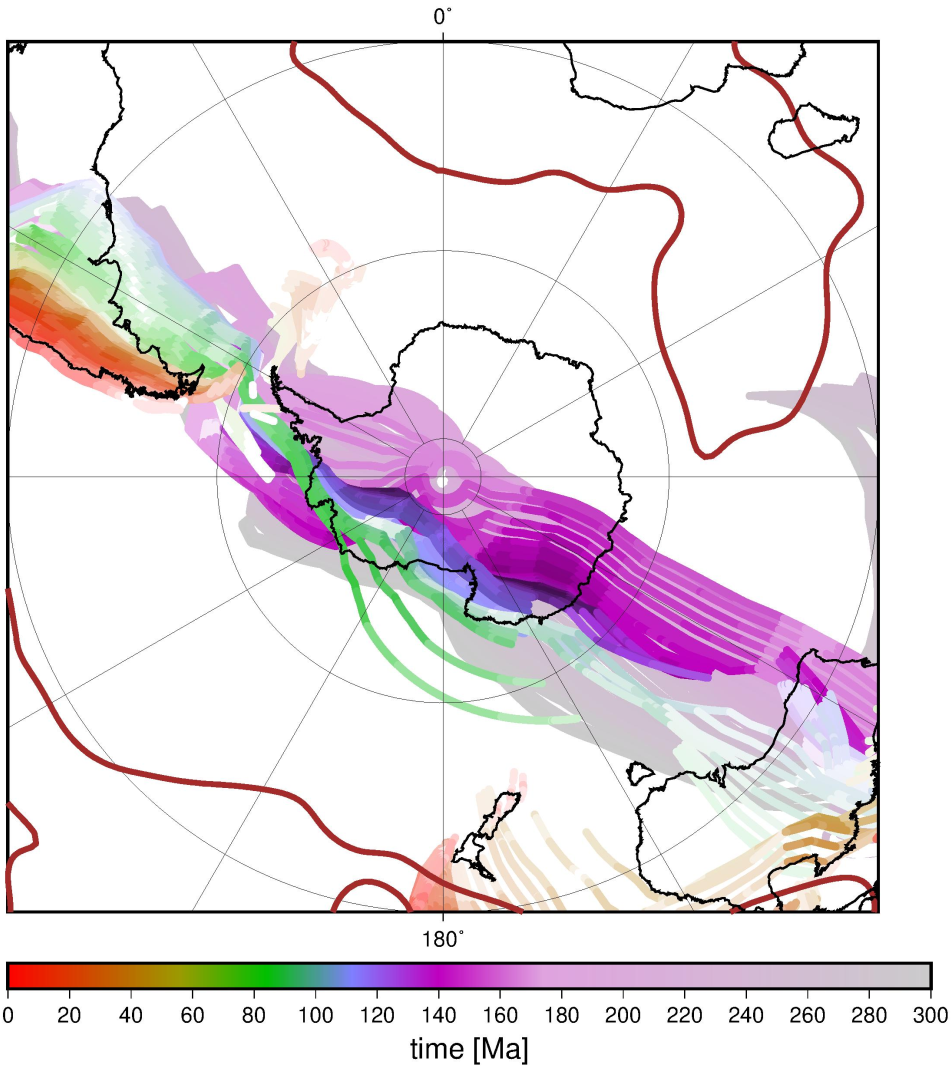

Figure 1. Locations of paleosubduction since 300 Ma from Antarctic perspective. After 140 Ma, higher subduction rates correspond to darker colors. See Steinberger et al. (2012) for details, in particular their Figure 2 for a complete color scale that also specifies how darkness relates to subduction rates. Brown line shows the -1% contour in the lowermost layer of SMEAN (Becker & Boschi 2002), an average over three tomography models, as a proxy for LLSVP margins.

mantle (van der Meer et al. 2010; Domeier et al. 2016), there is still a lot of sinking slab material beneath Antarctica, hence there is still overall downward flow expected in the region.

Figure 2 shows large-scale convective mantle flow (Hager & O'Connell 1979, 1981) based on a density model inferred from mantle tomography. Conversion from seismic velocity to density anomalies and radial viscosity structure is based on mineral physics; the latter additionally including constraints from geoid, heat flux and postglacial rebound (Steinberger & Calderwood

2006). Overall, it conforms to the expectations outlined in the previous paragraph: there is a belt of downward flow crossing Antarctica. Flow is mostly towards it in the upper part of the mantle, and away from it towards the base of the mantle. The belt of downward flow tends to be narrower in the upper part of the mantle. Upward flow extends from the Pacific towards parts of West Antarctica, whereas most of East Antarctica is underlain by downward flow. Although this result is for one particular tomography model, large-scale structure is rather consistently imaged throughout various recent tomography models, hence these features appear to be rather robust: even though there may still be slabs present in the upper $\sim$1000 km beneath Antarctica, especially beneath the Antarctic Peninsula (Lloyd 2018), upward flow may occur beneath the Ross Sea Embayment and Marie Byrd Land in the upper mantle, even above sinking slabs in the lower mantle. This could result if hot material has entered that region through horizontal flow in the upper mantle or tilted plume conduits (as discussed below) with its buoyancy counteracting negative buoyancy of slabs beneath. A similar setting is also likely present in the western United States. Horizontal flow in the upper mantle, shown here at depth 650 km, also exhibits more small-scale structure – in particular, flow across east Antarctica, towards the West Antarctic upper-mantle upwelling. At 2650 km depth, viscosity is higher and small-scale flow structures are less evident.

7.1.2 Mantle Convection and Dynamic Topography

Besides the geoid, dynamic topography – that is, how the lithosphere is pushed upwards above mantle upwellings and pulled down above downwellings (as sketched in Figure 3) – is another important prediction from mantle flow models (Yang & Gurnis 2016; Steinberger et al. 2019a). Amplitudes are of the order 1 km over regions extending several hundred to thousands of km, reaching maximal amplitudes of 2-3 km in some regions. It can be compared to observed topography, however, the comparison is not straightforward, as most of the topography is sustained by crustal thickness variations, which have to be corrected for and are uncertain. The corrected "residual topography" (e.g. Hoggard et al. 2016) hence has uncertainties on the order of 1 km. Figure 4 shows positive dynamic topography corresponding to upward flow in the upper mantle,

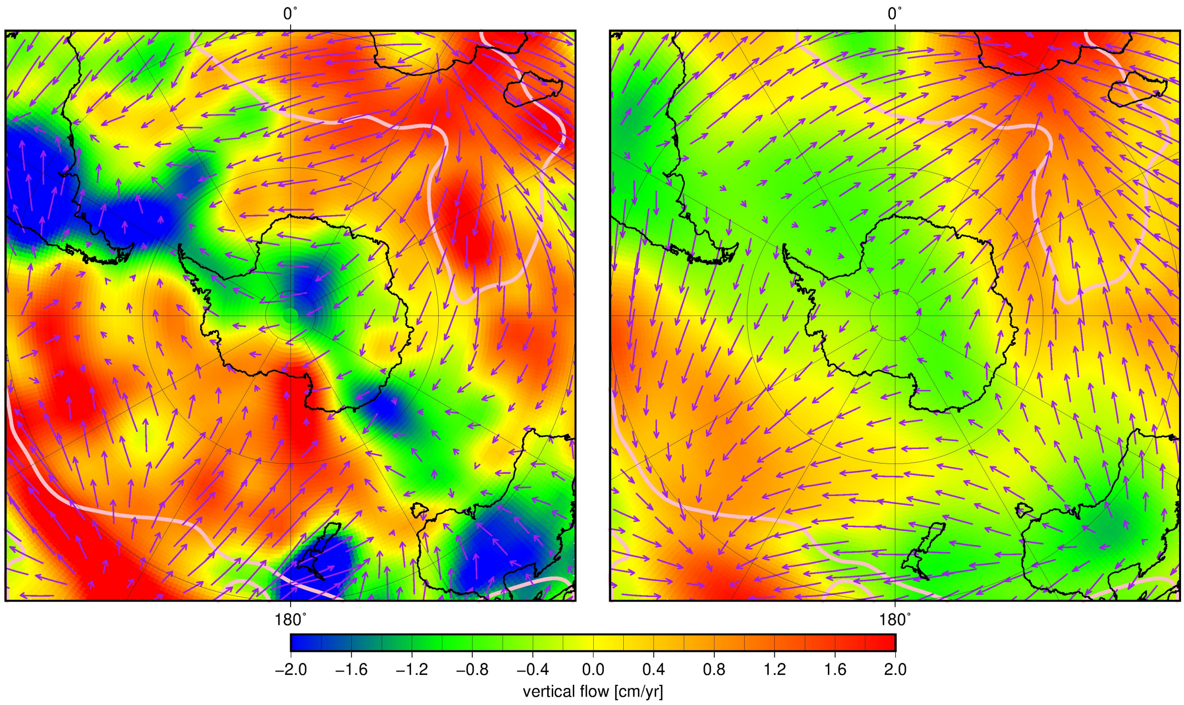

Figure 2. Computed global mantle convection flow field from Antarctic perspective, for S10MEAN (Doubrovine et al. 2016), an average over ten tomography models, considering chemically distinct LLSVPs – see Steinberger et al. (2019b) for details. Depth slices at 650 km (left) and 2650 km (right). Colors for vertical flow, arrows for horizontal flow. 1 cm/yr corresponds to 4 degrees of arc arrow length. Pink line shows the -1% contour in the lowermost layer of SMEAN (Becker & Boschi 2002) as a proxy for LLSVP margins.

beneath West Antarctica, whereas dynamic topography is mostly negative in East Antarctica, due to mostly downward flow beneath. This result only considers variations of viscosity with depth; lateral viscosity variations (LVV) are disregarded. Steinberger et al. (2019a) find that, if LVV due to temperature variations inferred from seismic tomography are considered, the dynamic topography pattern remains broadly similar, but the amplitude tends to be higher in continental regions, because thicker continental lithosphere tends to couple more strongly to underlying mantle flow than thinner oceanic lithosphere. Presence of a plume, as discussed in chapter 7.1.3, could cause a pronounced plume-fed low-viscosity zone in the shallow asthenosphere, partly decoupling the lithosphere from underlying mantle flow. Since such a decoupling layer is not present in our models, absolute amplitudes, in particular in plume-affected regions, could be somewhat too high in our models, while patterns are grossly correct. In East Antarctica, modelled thick lithosphere

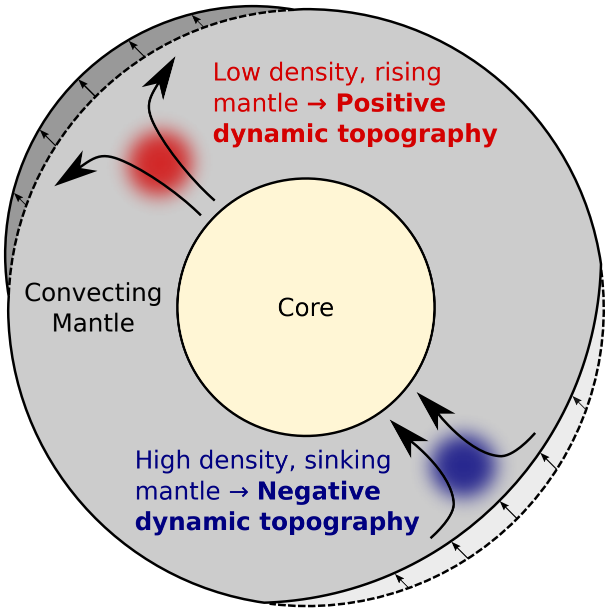

Figure 3. Low or high density anomalies in the mantle induce upward or downward mantle flow, which affects the surface as positive or negative dynamic topography, respectively. Sketch after Braun (2010).

leads to more pronounced negative dynamic topography, if LVV are considered. This makes it even more discrepant with observations-based estimates (Sleep 2006; Paxman this volume). the de-iced topography, which results from converting the ice sheet to an equivalent rock layer, is high in East Antarctica, and the inferred dynamic topography is positive. To explain this discrepancy, Sleep (2006) proposed a plume under East Antarctica, which might even have contributed to triggering Oligocene glaciation, in addition to the effect of declining atmospheric CO_2 (DeConto & Pollard 2003). Ponded plume material below the lithosphere could cause dynamic uplift, while possibly neither the plume conduit nor the layer of ponded low-velocity material could be seismically imaged, if they are rather thin. An alternative explanation for the high topography of East Antarctica could be that it did not erode much since the last orogeny, and that its crust is thicker than in the models that are used to subtract isostatic topography. For more details concerning specific Antarctic regions, see Paxman (this volume).

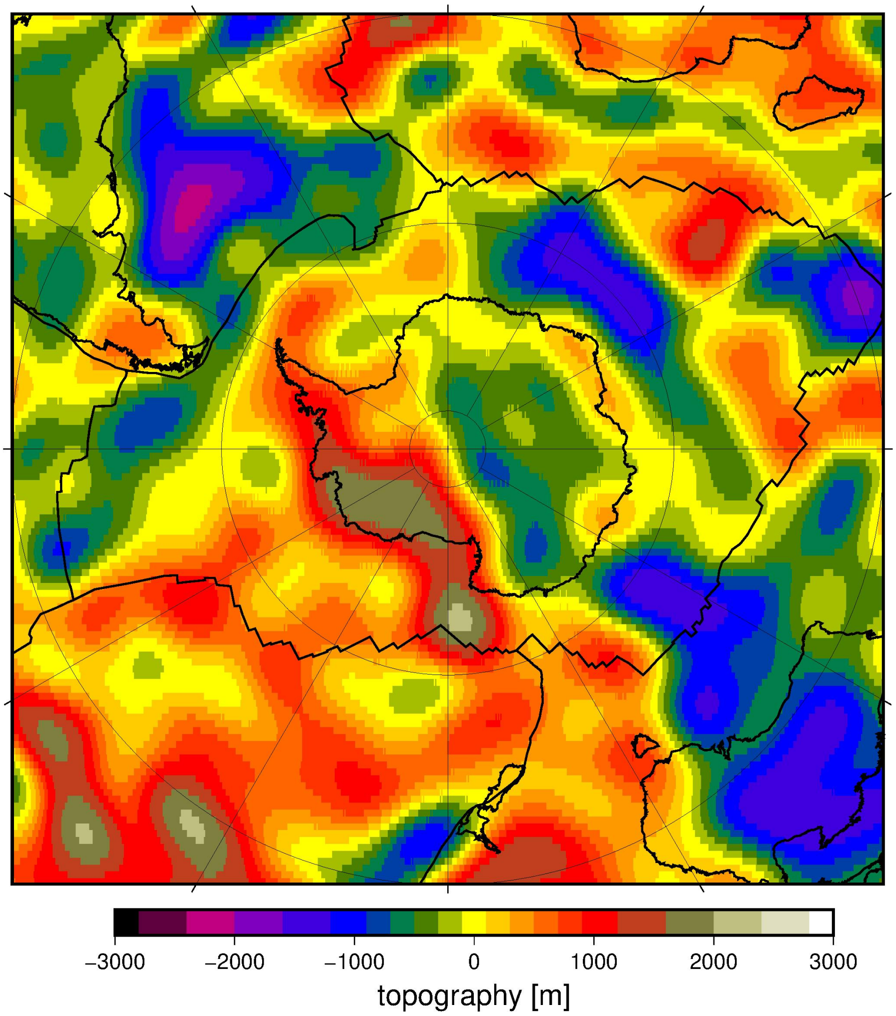

Figure 4. Model of dynamic topography from Steinberger et al. (2019a), case without lateral viscosity variations from Antarctic perspective.

7.1.3 Mantle Plumes

7.1.3.1 Classical and Modern Concepts of Mantle Plumes

Historically, the idea of steady plumes in the Earth's mantle started with surface observations in the Pacific Ocean, more precisely with the eye-catching Hawaiian-Emperor Seamount Chain. This strictly age-progressive line of seamounts, plateaus and islands is almost 6000 km long, linear (with the characteristic 60° bend), and ends close to Hawaii with its well-known volcanic activities. A stationary heat source within the mantle, above which the tectonic Pacific plate moved slowly over time, provides a simple and elegant explanation for the origin of these impressive and long-lived surface features and was first proposed by Wilson (1963).

This theory was later refined by Morgan (1971, 1972), who described mantle plumes as localized upwellings of hot, buoyant material rising from the core-mantle boundary (CMB) through the entire mantle up to the base of the lithosphere, where the material spreads laterally and pressure-release melting creates a volcanically active hotspot such as Hawaii at the surface. These central elements define what is nowadays referred to as the classical plume theory.

This theory has been revised and even entirely been questioned (e.g. Anderson & Natland 2005; Foulger 2011) several times since its original formulation, because mantle plumes are difficult to image. Therefore, the classical plume theory can neither be easily proved nor disproved.

However, evidence in favour of the existence of plumes has been provided by numerous laboratory experiments (e.g. Whitehead & Luther 1975; Griffiths & Campbell 1990) or numerical models (e.g. Farnetani & Richards 1995; van Keken 1997) that aim at investigating the basic principles of thermal convection and mantle dynamics (see Figure 5). These studies consistently demonstrate that hot, buoyant upwellings (such as plumes) and cold, dense downwellings (such as subduction zones) are natural and dynamic counterparts of any convecting system, and can therefore also be expected in the Earth's mantle.

Concerning the shape of mantle plumes, both laboratory and numerical models indicate that thermal plumes initially consist of a large, spherical plume head, subsequently supplied by a cylindrical, narrow and long plume tail (see Figure 5). This head-and-tail structure results in two very different surface effects: plume heads initiate voluminous eruptions that create gigantic flood basalt provinces within the relatively short duration of a few million years (Large Igneous Provinces, abbreviated LIPs and defined by Bryan & Ernst (2008) as "magmatic provinces with areal extents $> 0.1 \times 10^6$ km^2, igneous volumes $> 0.1 \times 10^6$ km^3 and maximum lifespans of $\sim$50 Myr that have intraplate tectonic settings or geochemical affinities, and are characterised by igneous pulse(s) of short duration ($\sim$1 – 5 Myr), during which a large proportion ($>75\%$) of the total igneous volume has been emplaced"). Plume tails, on the contrary, can easily be active for more than a hundred million years, produce substantially less magma and create an

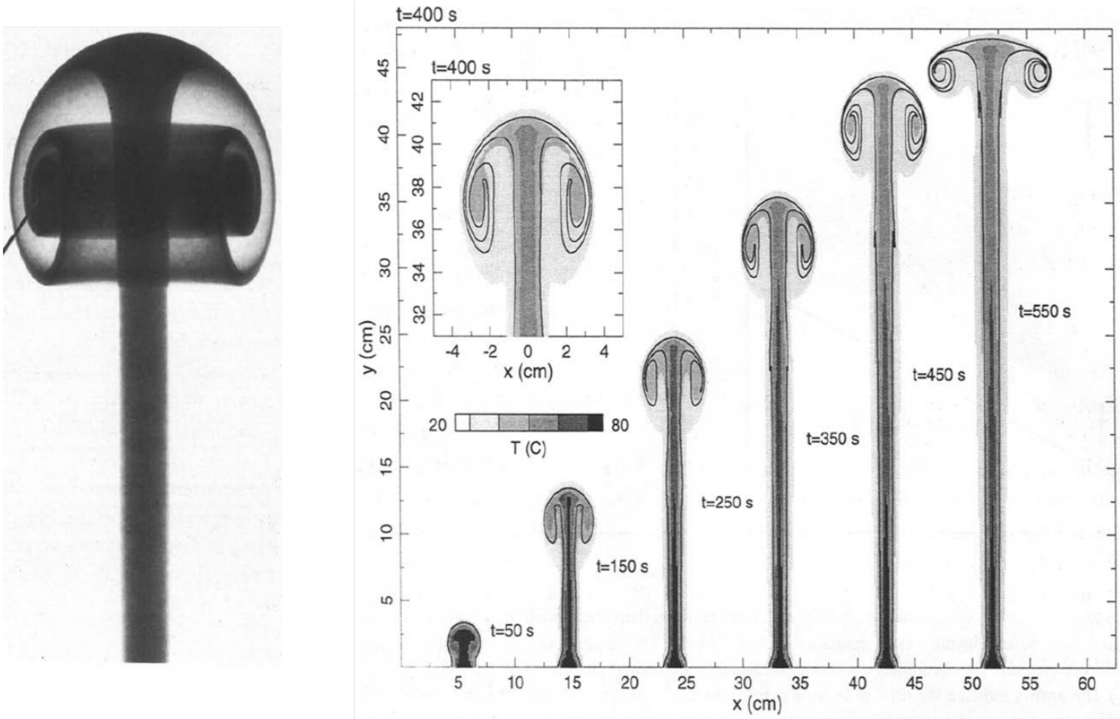

Figure 5. Both laboratory experiments with highly viscous glucose syrup (left, from Griffiths & Campbell 1990) and two-dimensional numerical models (right, from van Keken 1997, and with laboratory scaling) showed early on that upwelling plumes generally look like a mushroom – with a big, spherical head and a thin, vertical tail. Our results in section 7.1.3.4 suggest that for a potential plume under West Antarctica, the head rise time translates to $\sim$30 - 60 Myr, with large uncertainty, for mantle scales.

age-progressive hotspot track when the lithosphere moves above the relatively stationary plume (Richards et al. 1989). Both plume heads and tails have reshaped substantial areas on the Earth's surface (see Figure 6).

Note that apart from the interaction with the mobile tectonic plates, the amount of volcanic products also depends on the relief of the base of the lithosphere, since hot material can flow buoyantly upward and pond beneath regions of thinner lithosphere. This process is known as upside-down drainage (Sleep 1997) and emphasizes the importance of considering local lithosphere thickness variations, because melting and the associated hotspot do not necessarily occur vertically above the plume centre.

The term hotspot is rather vaguely defined as a localized surface region where volcanic activities take place over a long time and independent of any plate tectonic processes (e.g. Schubert et al. 2001). Therefore, different catalogues list different hotspots, usually between 40

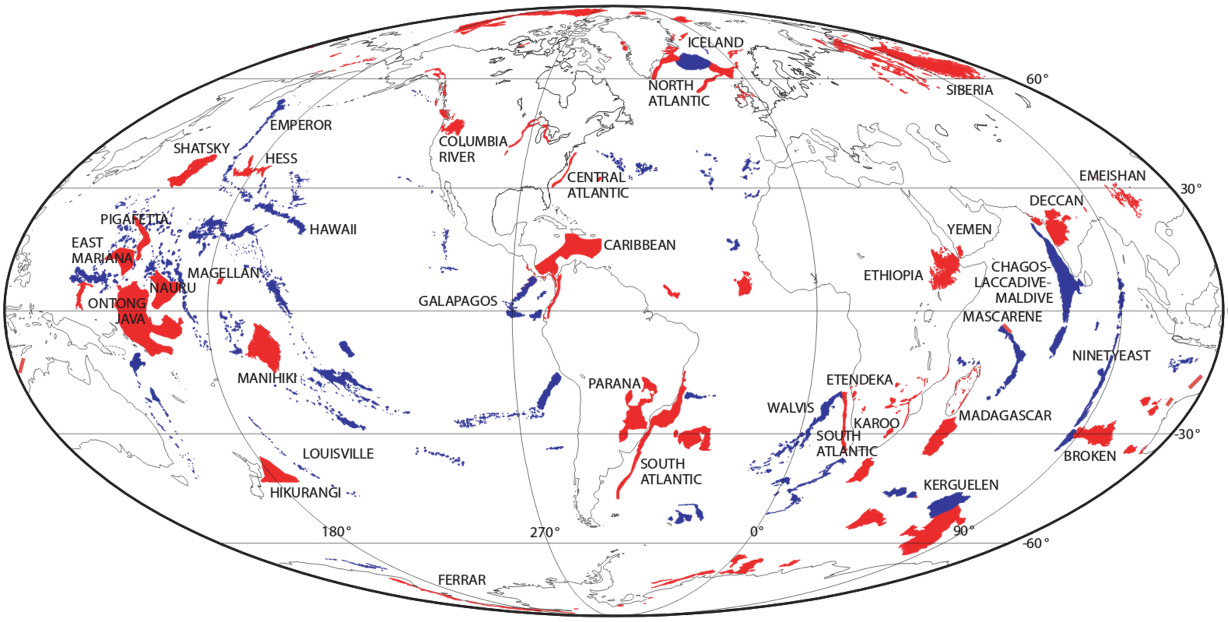

Figure 6. Overview of LIPs (red) and hotspot tracks (blue), demonstrating the extent of the areas on Earth's surface that have been affected by plume heads and tails, respectively, over many millions of years – in some cases for more than a hundred million years. The only onshore LIP marked in Antarctica is the ca. 180 Myr old Ferrar LIP, which follows the Transantarctic Mountains along nearly 3500 km (Elliot & Fleming 2004). Offshore, there is also the Kerguelen LIP on the Antarctic plate. The volcanic province in West Antarctica (see chapter 7.1.3.2) is not shown. Figure from Coffin et al. (2006) (licensed under CC BY 4.0; https://creativecommons.org/licenses/by/4.0/).

and 50, depending on the applied criteria (e.g. Steinberger 2000; Courtillot et al. 2003; King & Adam 2014). Generally accepted factors for hotspots possibly fed by deep mantle plumes are the occurrence of a LIP, a clearly age-progressive hotspot track in accordance with the reconstructed directions and velocities of the moving plates as well as ongoing magmatic activities at the current hotspot location, surrounded by a broad topographic hotspot swell (e.g. Courtillot et al. 2003). Furthermore, the geochemical signature of hotspot-derived rock samples resembles that of ocean-island basalts while being distinctly different from other basalts produced at mid-ocean ridges (e.g. Moreira & Allègre 1998), and the plume requires a certain buoyancy to be able to ascend through the entire mantle (e.g. Steinberger & O'Connell 1998). Hotspots can be active for many tens of millions of years; for example, the Kerguelen hotspot has been persistently active for ca. 130 Ma (Coffin et al. 2002).

As mentioned above, plumes are difficult to image. Seismic tomography is theoretically able

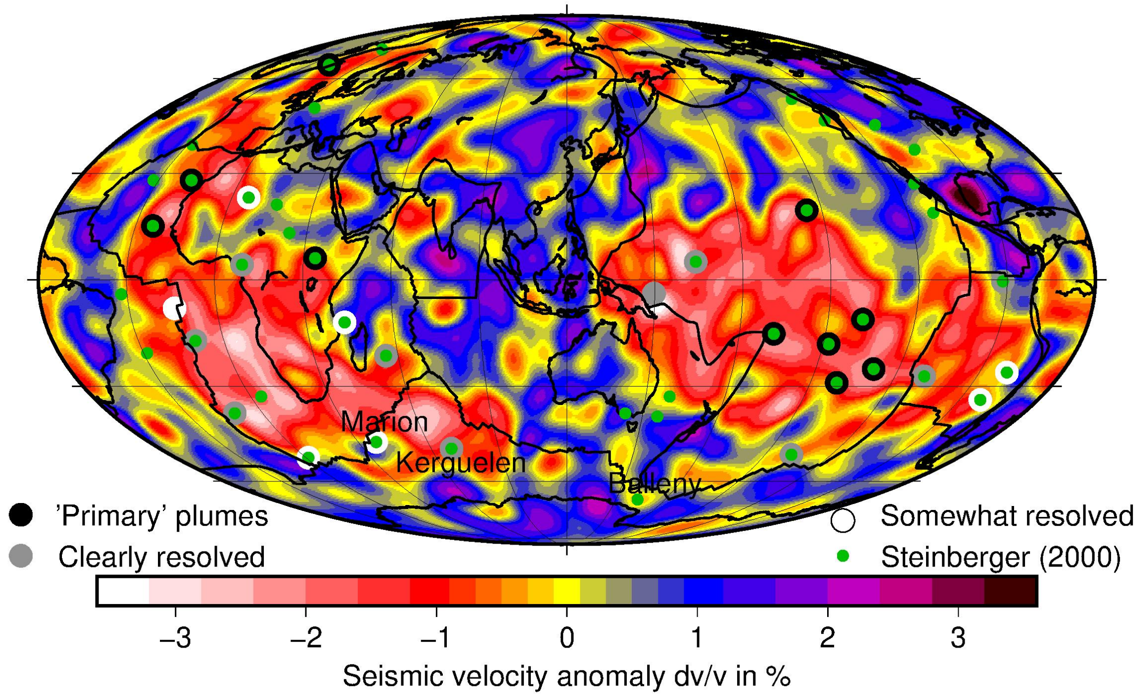

Figure 7. Hotspot locations after Steinberger (2000) (all green dots) where the hotspots underlain by vertically continuous conduits in the lower mantle in the seismic tomography model of French & Romanowicz (2015) are marked as primary or clearly resolved plumes (black and grey circles, respectively). White circles are for somewhat resolved plumes. The background colours show the tomography model at 2800 km depth, which highlights the two zones of extremely slow anomalies, the African and Pacific LLSVPs (the two broad red areas). The only hotspot in vicinity of Antarctica are the Balleny Islands (south of New Zealand) – which lack even a somewhat resolved conduit and are far away from the closest LLSVP. The Kerguelen and Marion plumes (clearly and somewhat resolved, respectively) are also beneath the Antarctic plate, close to the southern margin of the African LLSVP, however far from the continent. Figure redrawn after French & Romanowicz (2015).

to detect regions of reduced seismic velocities. The technique is however strongly limited by the available ray coverage and the rapidly decreasing resolution with depth, which make it extremely challenging to capture rather narrow plume conduits. A few years ago, French & Romanowicz (2015) provided the first convincing and long-awaited whole-mantle tomography images that do resolve continuous slow velocity structures throughout the entire mantle (see Figure 7 for their global distribution). The deep roots of the plumes at the core-mantle boundary appear however to be much broader than expected and the highy deflected plume tails above approximately 1000 km depth deviate significantly from the classically predicted vertical conduits.

Additional geometrical discrepancies with respect to the classical plume concept comprise deformed, asymmetrical plume heads and highly tilted plume tails, which may result from an asymmetric relief of the base of the lithosphere, interactions with the lithosphere moving above the plume, large-scale asthenospheric flow surrounding (and possibly deflecting) the plume or, in particular, interactions with nearby spreading ridges (as for example shown for the Réunion plume in the geodynamic models of Bredow et al. (2017) or the surface wave tomography model of Mazzullo et al. (2017)).

Regarding the source location, plumes are assumed to start from instabilities at thermal boundary layers such as the CMB. More precisely, reconstructed eruption sites of LIPs and present-day hotspot positions seem to indicate that deep plumes are generated at the margins of the African and Pacific LLSVPs (Torsvik et al. 2006; Burke et al. 2008), defined as the -1% shear wave velocity contour of the SMEAN composite tomography model (Becker & Boschi 2002). The choice of this specific contour is however rather arbitrary and the statistical significance of the spatial correlation can be questioned (Austermann et al. 2014). This means that the entire seismically slow zones in the lowermost mantle – and not just their margins – could be potential plume generation zones, located approximately beneath the African continent and the central Pacific Ocean. Moreover, the global tomography model of Hosseini et al. (2019) images the LLSVPs for the first time also in a P-wave model, such that the term LLVP (without the "shear") becomes more appropriate. Interestingly, the two large and continuous provinces that were consistently seen in previous shear wave models, appear in the P-wave model as numerous patches, which form an almost continuous global belt slightly south of the equator. However, in any case, the regions in which deep plumes start their ascent through the mantle are located rather far away from Antarctica (see Figure 7).

7.1.3.2 West Antarctic Mantle Plume Hypothesis

From a global geodynamic perspective, West Antarctica seems to be a rather unlikely location to observe the surface manifestations of a mantle plume (Sleep 2006) and unsurprisingly, it has never been included in any global hotspot catalogue so far (e.g. Steinberger 2000; Courtillot et al. 2003; King & Adam 2014, see also chapter 7.1.3.1).

Nonetheless, a broad structural dome, resembling a hotspot swell, has been recognized in Marie Byrd Land, based on sub-glacial bedrock topography corrected for ice loading (Paxman et al. 2019). Additionally, the geochemical characteristics of basaltic rocks throughout West Antarctica are similar to those of plume-related ocean island basalts and most likely originate from a depleted mantle source from depths of at least 100 km (see also Handler et al. this volume). Thus, the West Antarctic Ice Sheet might conceal an extensive LIP. Behrendt et al. (1992) were the first to link and explain these observations with a plume underneath West Antarctica, more precisely an ellipsoidal plume beneath the West Antarctic Rift System with a major axis of about 3000 km length. This suggested plume area comprises the entire Marie Byrd Land, the West Antarctic Rift System, the Ross Ice Shelf, and even Northern Victoria Land – exceeding by far the dimensions of the largest known plumes on Earth such as Hawaii or Iceland.

Another study, which was published in the same year, focused on the petrology of lavas from the still active Mount Erebus volcano on Ross Island (Kyle et al. 1992), which also seem to be derived from a depleted asthenospheric mantle source without much crustal contamination. The authors concluded that a relatively small plume centered beneath Mount Erebus with a diameter of 40 km and a rising rate of 6.5 cm/yr would be sufficient to account for the estimated volume of volcanic material necessary to build Mount Erebus and the neighboring volcanoes – values more within the range of classical plume parameters. However, there are also xenoliths representing young lithosphere (Day et al. 2019).

Ever since, the hypothesis of a mantle plume beneath West Antarctica (most often considered either beneath central Marie Byrd Land or Ross Island rather than beneath entire West Antarctica) has been subject to detailed studies from various geoscientific disciplines. The most abundant indications at the surface (wherever rocks are exposed) are the widely spread basalts, which have been found throughout West Antarctica (LeMasurier & Rex 1989). Having been produced continuously over the past 30 Myr, they do not follow a classical age-progressive hotspot track over hundreds of kilometers or even a single chain of volcanoes. This is however no striking argument against a plume, considering that the Antarctic plate has been virtually immobile over the past 85 Myr (Larter et al. 2002).

Altogether, Marie Byrd Land hosts 18 big alkaline shield volcanoes, with volumes of up to 1,800 km^3, and distributed over the approximately 500 x 800 km large tectonic dome (LeMasurier 2013). Additionally, a recent study found indications for up to 138 individual conical bedrock edifices beneath the thick ice sheets, based on combining aeromagnetic, aerogravity and satellite data (de Vries et al. 2018). These potential volcanoes are distributed across the entire rift system, including the area of extended continental crust where no volcano had previously been reported. Whether a few or all of the conical bedrock topography edifices do have a volcanic origin or not – the West Antarctic subglacial volcanic province is undoubtedly one of the largest volcanic provinces in the world. However, regarding the plume hypothesis, it remains uncertain if the volcanoes form a LIP, which means that conclusive proof for the surface manifestation of a plume head is still missing.

For the sake of completeness, it should be noted that there is also another, much older LIP in Antarctica: the Ferrar LIP (Elliot & Fleming 2004), emplaced at 183 Ma (Burgess et al. 2015) along 3500 km of the Transantarctic Mountain range (shown in Figure 6). It is however neither related to the volcanic province nor to the plume in West Antarctica.

As mentioned above, the geochemical signature of the volcanic rocks in West Antarctica can hardly be distinguished from ocean island basalts and they seem to be derived from mantle depths (e.g. LeMasurier & Rex 1989; Panter et al. 2018; Martin et al. 2013), strongly suggesting the influence of a deep plume. Further geochemical evidence for mantle plume components has been found in various studies for both Ross Island and Marie Byrd Land (Rocholl et al. 1995; Panter et al. 1997, 2000; Phillips et al. 2018; Hole & LeMasurier ; Panter et al. 2000). However, Helium isotope data have been used to argue against a plume origin (Nardini et al. 2009; Day et al. 2019)

An increasing amount of seismic data provides evidence that large zones of slow seismic velocities exist both underneath Marie Byrd Land and Ross Island and could be signs of possible plume structures (e.g. Accardo et al. 2014; Hansen et al. 2014; Lloyd et al. 2015; Shen et al. 2018, see also Wiens et al. this volume). Assuming that these seismic anomalies are temperature-driven, and not caused by the presence of fluids such as water or a different material composition, the potential plume structures can be followed at least down to the transition zone. At depths greater than 800 km, poor resolution impedes any clear findings. One of the most recent Antarctica-wide studies, by Lloyd (2018), concludes that the seismic anomaly beneath Marie Byrd Land (centered near Mount Sidley) may indeed indicate the existence of a mantle plume, whereas the presence of a potential plume beneath Mount Erebus remains elusive. Convincing proof for deep plume structures beneath West Antarctica is still lacking.

Another physical parameter indicating potential plume activities beneath West Antarctica is the elevated heat flux in West Antarctica, either measured at the bedrock surface or calculated in continent-wide heat flux models (Pappa & Ebbing this volume) or inferred from mantle xenoliths (Martin et al. this volume; Handler et al. this volume; Casetta et al. this volume). The surface heat flux has been estimated from global seismic models comprising the crust and upper mantle (Shapiro & Ritzwoller 2004), from satellite magnetic data (Fox Maule et al. 2005), from a continental shear velocity model (An et al. 2015) or from airborne magnetic data (Martos et al. 2017) as shown in Figure 8. Even though direct measurements are sparse and the models result in rather different value ranges and anomalies, the heat flux in West Antarctica is always distinctly elevated compared to the values above cratonic East Antarctica with its thick crust and lithosphere. More or less clearly pronounced anomalies appear in Marie Byrd Land and in the vicinity of Ross Island, following the Transantarctic Mountain chain, which could be interpreted as plume-related surface manifestations, due to additional heat supply caused by plume material ponding beneath the lithosphere. This scenario has recently been tested in numerical models by Seroussi et al. (2017) in the context of the plume-induced heat flux at the base of the ice sheet, concluding that a plume with moderate parameters is certainly possible beneath Marie Byrd Land.

Additionally, the possible presence of a plume under East Antarctica (already discussed in chapter 7.1.2) needs to be considered here: Plume material may spill across the Transantarctic Mountains from beneath thicker East Antarctic lithosphere towards beneath thinner West Antarc-

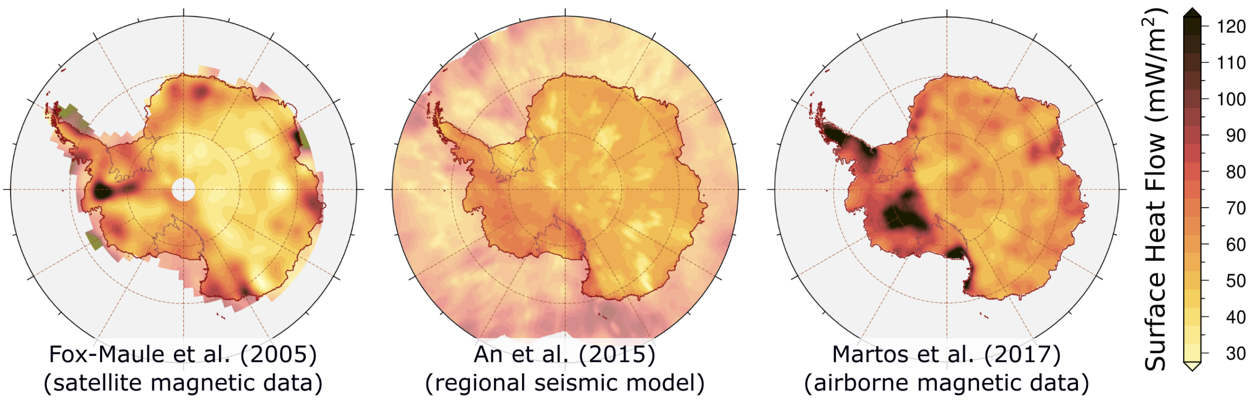

Figure 8. Previous heat flux estimates derived either from magnetic or seismic data consistently show an elevated heat flux beneath West Antarctica in contrast to East Antarctica (Data from Fox Maule et al. 2005; An et al. 2015; Martos et al. 2017). Since the focus is on the continent, the colours in the oceanic areas are slightly dimmed.

tic lithosphere (Sleep 2006) leading to pressure-release melting. Like beneath Africa (Ebinger & Sleep 1998), a single plume could possibly lead to distributed magmatism throughout a wide area, due to lateral flow and ponding of plume material in pre-existing zones of lithospheric thinning.

Putting together all indications for the presence of one or even two potential mantle plumes beneath West Antarctica, it becomes clear that without any direct evidence for a LIP, an age-progressive hotspot track or a possible plume origin at greater depths, it is practically impossible to constrain the dynamic history of the plume(s) without a considerable amount of speculation. To complicate the situation, there is a variety of alternative explanations for the intraplate volcanism, such as the presence of water or other fluids in the upper mantle instead of a thermal anomaly, and in the case of Ross Island, there might also be edge-driven or edge-modulated convection effects (King 2007; Sleep 2007; Panter et al. 2018) at the pronounced step in the lithosphere thickness along the Transantarctic Mountain chain (van Wijk et al. 2008), or there might be rift- or transtension-related decompression melting (Cooper et al. 2007; Rocchi et al. 2003, 2005). Also, in contrast to the Marie Byrd Land dome, Ross island is located in a depression.

7.1.3.3 Geodynamic Models of a West Antartic Mantle Plume

Although the existence of a mantle plume beneath the West Antarctic lithosphere remains uncertain (see chapter 7.1.3.2 for details), it is still useful to study geodynamic models of plumes beneath that region, and which predictions of such models could possibly be compared to observations.

Given the lack of time-dependent observations such as an age-progressive distribution of volcanoes, instantaneous models (which only consider the present-day situation and are de facto not truly "dynamic") seem to be a reasonable choice. The comparatively well-confirmed anomalies of low seismic velocities in the crust and upper mantle can be used as constraints. Furthermore, the recently developed three-dimensional model of the Antarctic lithosphere by Pappa et al. (2019) provides continuous regional information about the laterally varying crustal and lithospheric thickness. Model details can be found in Pappa and Ebbing (this volume).

The mantle convection code ASPECT, short for Advanced Solver for Problems in Earth's ConvecTion, (Kronbichler et al. 2012; Heister et al. 2017), and originally intended for simulations of time-dependent convection models, can be used to solve only the energy equation. Usually, the compressible Stokes equations also need to be solved for geodynamic models, but all time-dependent terms can be neglected if the material inside the model domain is not assumed to be moving. In this case, the energy equation is iteratively solved until the temperature field has reached a steady state.

As input parameters, the model requires the spatial distribution of temperatures and compositions. Each composition has a certain density, specific heat capacity, thermal conductivity and specific radiogenic heat production rate, all taken from the lithosphere model of Pappa et al. (2019). In order to test the plume hypothesis, a spherical hot anomaly (in the shape of a Gaussian spherical distribution) with a certain excess temperature and width is inserted into the model, either beneath Marie Byrd Land or Ross Island (Figure 9). The excess temperature is chosen in agreement with literature estimates for other plumes: between 100 and 250 K (e.g. Schilling 1991; Putirka 2008), whereas the width approximately fits the extent of the seismic anomalies: between 150 and 250 km (Lloyd 2018).

Besides a steady state for the temperatures, the model provides the heat flux at the bedrock surface, beneath the ice sheets (an input parameter of major importance for Glacial Isostatic Adjustment models, see also Barletta and Nield this volume). The final model output represents

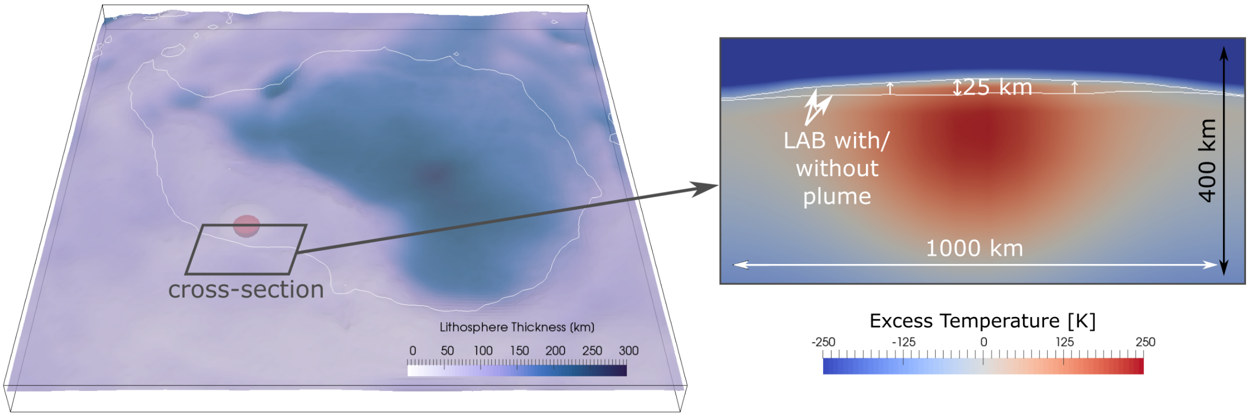

Figure 9. Lithosphere thickness distribution in the ASPECT model with the inserted spherical thermal anomaly that simulates a plume beneath Marie Byrd Land with a maximum excess temperature of 250 K (left); the white line shows the outline of Antarctica. Cross-section of the thermal anomaly and the resulting uplift of the LAB (right).

an estimation of the additional heat flux that would be contributed by a plume-sized thermal anomaly either beneath Marie Byrd Land or Ross Island.

The results show that the lithosphere-asthenosphere boundary (LAB) is affected by the plume anomaly over a maximum diameter of 1000 km and shifted upwards up to 25 km (Figure 9), in good agreement with previous models of plume-lithosphere interactions (Bredow et al. 2017). The additional heat flux signature caused by the thermal (plume) anomaly reaches values between 7.1 and 14.0 mW/m^2, with a diameter between 600 and 1290 km (Figure 10). The shape of the plume heat flux signature is not consistently circular, pointing out the importance of considering local lithosphere thickness variations. This is especially important in the case of the Ross Island plume, since it is very close to the sudden step in the lithosphere thickness along the Transantarctic Mountains. Altogether, the changes of the heat flux caused by the plume seem to be rather small. It should however be noted that these calculations only consider the conductive heat transfer and neglect any heat transport via volcanic activities that are definitively present in these areas.

Overall, the results do not disagree with previous studies of the surface heat flux, especially given the discrepancies between these studies (see Figure 8). Evaluated solely from these models, neither position can be ruled out nor confirmed as a potential location for a plume.

It is noteworthy that the parameters used for the simulations have an impact on the results, for example if the shape of the plume anomaly is pancake-like rather than spherical. The resulting difference is, however, most likely very small and since not even the presence of a plume can be confirmed, constraining its shape seems impossible at the moment and with this specific model setup. Another critical parameter is the lithosphere model by Pappa et al. (2019), which is used as input configuration. The distribution of compositions and temperatures, in particular the depth of the lithosphere-asthenosphere boundary, certainly has an impact. Unfortunately, there is no similarly well-resolved model of Antarctica available at the moment, such that there is no alternative to the lithosphere model by Pappa et al. (2019) so far.

7.1.3.4 Modelling Plume Conduits beneath Antarctica

Another approach to investigate a potential plume beneath West Antarctica with geodynamic models tackles the question of its origin. Assuming that the zones of low seismic velocities beneath Marie Byrd Land or Ross Island reflect thermal anomalies, this hot material must either have been heated at its current position via tectonic process(es) or buoyantly risen from greater depths (like a deep mantle plume). In the latter case, geodynamic models can be used to assess the likelihood that a plume has risen towards a specific surface position within the global mantle flow pattern, which is known to deflect plumes.

The procedure of Steinberger et al. (2019b) models the ascent of plume heads and tails with a certain rising speed and embedded in a time-dependent mantle flow field. The SMEAN tomography model (Becker & Boschi 2002) provides seismic velocities that can be converted into mantle densities (Steinberger & Calderwood 2006). Further input parameters are a radial viscosity structure (Steinberger & Calderwood 2006) and time-dependent plate motions (Torsvik et al. 2010), which enable the reconstruction of large-scale mantle flow. Time-dependence is also achieved by backward-advecting the density heterogeneities. In the specific case of West Antarctica, the plume is assumed to have reached the surface at 30 Ma, approximately simultaneously with the onset of volcanic activities. Both positions underneath Marie Byrd Land and Ross Island have been tested.

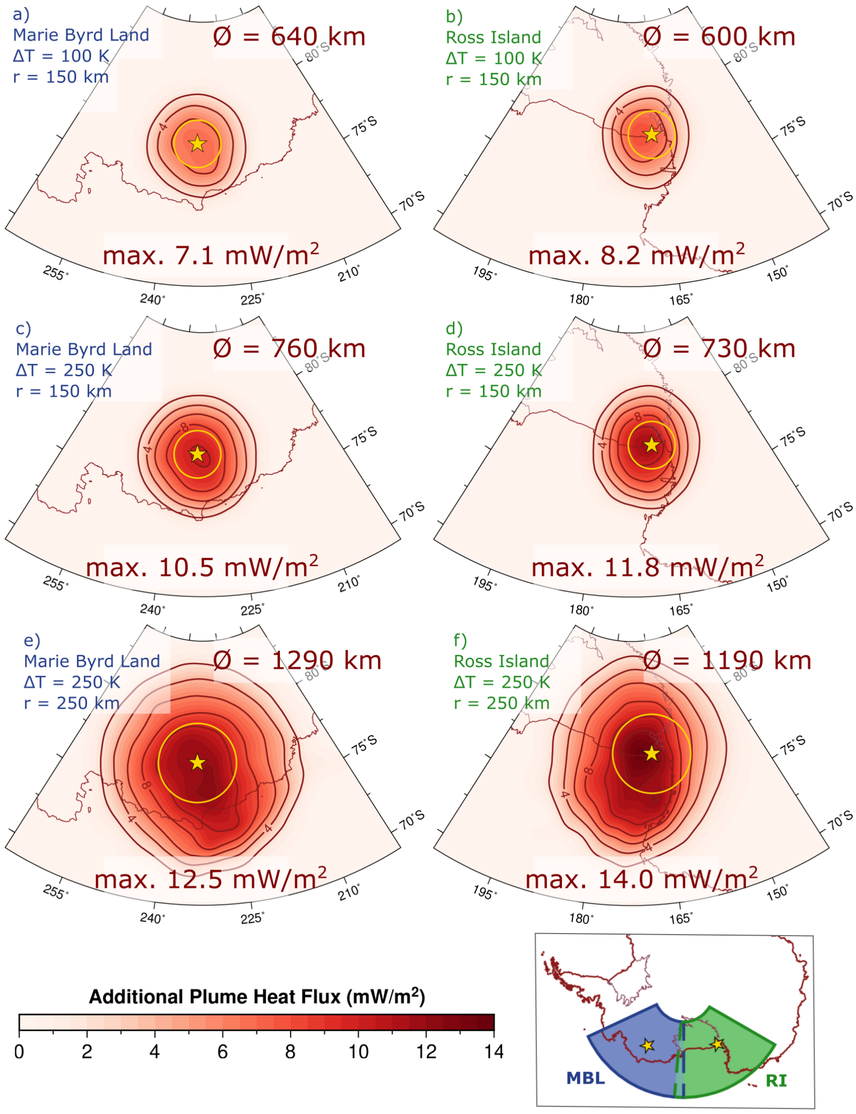

Figure 10. Additional heat flux signatures of a thermal plume with a radius of 150 km (a-d), or 250 km (e,f), variable plume excess temperatures of 100 K (a,b) or 250 K (c-f) and located beneath Marie Byrd Land (a,c,e) or Ross Island (b,d,f). Yellow stars and circles denote the positions and outlines of the modeled thermal anomalies. The inset map shows the positions of the two model regions. The diameter is calculated as the average value of the 2 mW/m^2 contour.

The model result shows the present-day state of the plume conduit, with its deflection by mantle flow discussed earlier in the paper and the location in the D'' layer at the base of the mantle from which it needs to start rising in order to reach the chosen surface position. It also shows if it is possible at all to generate a stable plume conduit underneath the surface position of interest. For Marie Byrd Land and Ross Island, stable plume conduits are possible, if the plume head takes up to 60 or 30 Myr, respectively, to rise through the entire mantle – but not if it takes any longer. Both values are however in a realistic range, between other recent estimates. Whereas Torsvik et al. (2020) find rise times of 30 Myr or less for plumes in the vicinity of LLSVPs (where the mantle is probably comparatively hot, less viscous and with predominantly rising flow), Steinberger et al. (2019b) find ∼80 Myr or longer for the Yellowstone plume head, rising far from LLSVPs, in the vicinity of sinking slabs. Figure 11 shows the case in which each plume head needs 30 Myr to ascend. Not surprisingly, and in accordance with seismic tomography images, the intrinsically vertical plume conduits are strongly tilted due to the complex flow pattern of the convecting mantle beneath Antarctica. The plumes start their ascent from the direction of the Pacific LLSVP, however still far away from its margin or the known deep plumes (red circles).

Altogether, it can be summarised that it is not unlikely for hot material to flow towards and ending up underneath Marie Byrd Land or Ross Island considering the directions and vigour of the mantle wind. A deep plume origin, with a highly tilted plume conduit can therefore not be ruled out, in agreement with available seismic images.

The models are however not suited to finally confirm the existence of a whole-mantle plume. For that purpose, seismic tomography models with a higher resolution at greater depths are the most promising – if not the only – tool to provide a conclusive answer. Until then, the debate about a potential plume beneath West Antarctica will continue.

ACKNOWLEDGMENTS

This work was supported by the European Space Agency (ESA) as part of the Support to Science Element (STSE) "3D Earth - A Dynamic Living Planet". The datasets used to perform the modeling in the current study are available along with the original studies as referenced (Fox Maule et al. 2005; An et al. 2015; Martos et al. 2017; Pappa et al. 2019). The geodynamic models in section 7.1.3.3. were computed with the open-source software ASPECT (https://aspect.geodynamics.org/) and we thank the Computational Infrastructure for Geodynamics (geodynamics.org) which is funded by the National Science Foundation under award EAR-0949446 and EAR-1550901 for supporting the development of ASPECT. Large-scale mantle flow (Figure 2), dynamic topography (Figure 4) and plume conduits in section 7.1.3.4 were computed

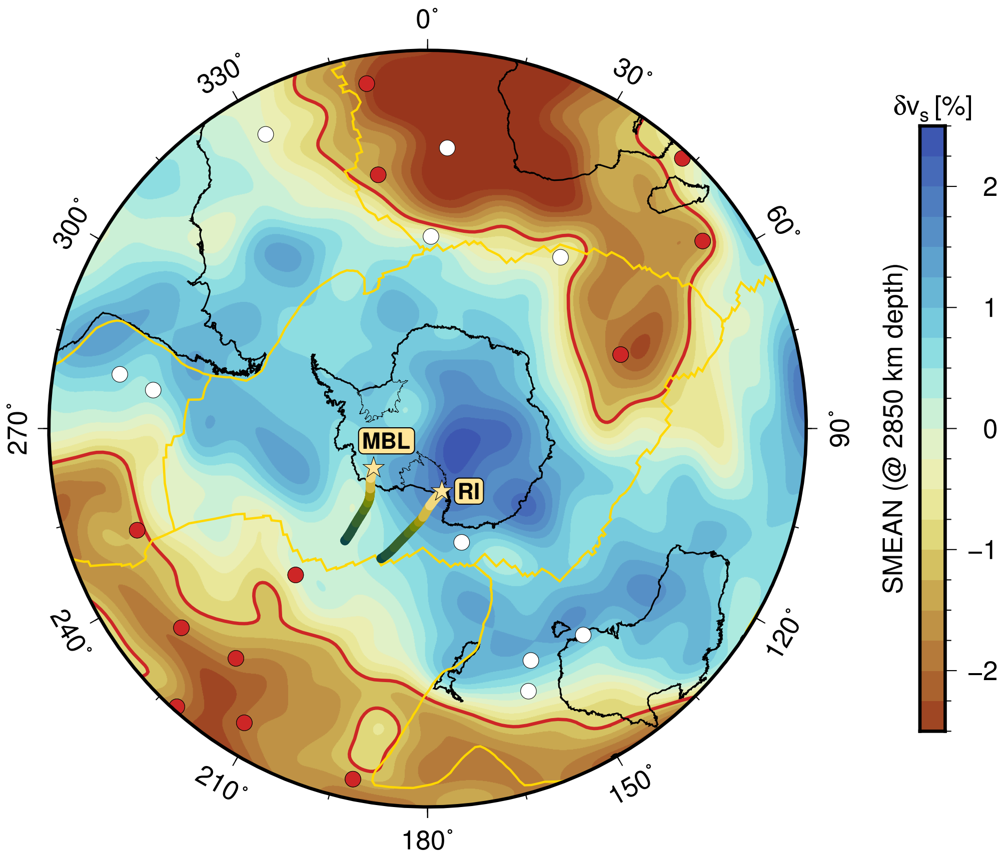

Figure 11. SMEAN tomography model (Becker & Boschi 2002) at the CMB from the Antarctic perspective. The two LLSVPs are visible as brown areas, framed by the -1% shear wave velocity contour (red line). All red and white circles denote the positions of the hotspots catalogued by Steinberger (2000), with red circles showing the primary and clearly resolved plumes detected by French & Romanowicz (2015). Yellow lines indicate plate boundaries. Stars show the locations of the potential plumes beneath Marie Byrd Land (MBL) or Ross Island (RI), underneath which the stability of whole-mantle plume conduits within the large-scale flow field was modelled. The pathways of the conduits are shown from the CMB up to the surface (colour-coded from dark to light green over depth).

with code available from B.S. upon request. The constructive comments by Norm Sleep, an anonymous reviewer and the Volume Editor, Wouter van der Wal, have been appreciated.

REFERENCES

Accardo, N. J., Wiens, D. A., Hernandez, S., Aster, R. C., Nyblade, A., Huerta, A., Anandakrishnan, S., Wilson, T., Heeszel, D. S., & Dalziel, I. W., 2014. Upper mantle seismic anisotropy beneath the West Antarctic Rift System and surrounding region from shear wave splitting analysis, *Geophysical Journal International*, **198**(1), 414–429.

An, M., Wiens, D. A., Zhao, Y., Feng, M., Nyblade, A., Kanao, M., Li, Y., Maggi, A., & Lévêque, J.-J., 2015. Temperature, lithosphere-asthenosphere boundary, and heat flux beneath the Antarctic Plate inferred from seismic velocities, *Journal of Geophysical Research: Solid Earth*, **120**(12), 8720–8742.

Anderson, D. L. & Natland, J. H., 2005. A brief history of the plume hypothesis and its competitors: concept and controversy, *Geological Society of America Special Papers*, **388**, 119–145.

Austermann, J., Kaye, B. T., Mitrovica, J. X., & Huybers, P., 2014. A statistical analysis of the correlation between large igneous provinces and lower mantle seismic structure, *Geophysical Journal International*, **197**(1), 1–9.

Becker, T. W. & Boschi, L., 2002. A comparison of tomographic and geodynamic mantle models, *Geochem., Geophys., Geosys.*, **3**, 1003.

Behrendt, J. C., LeMasurier, W., & Cooper, A. K., 1992. The West Antarctic Rift System – a propagating rift "captured" by a mantle plume?, *Recent Progress in Antarctic Earth Science*, pp. 315–322.

Braun, J., 2010. The many surface expressions of mantle dynamics, *Nature Geoscience*, **3**(12), 825–833.

Bredow, E., Steinberger, B., Gassmöller, R., & Dannberg, J., 2017. How plume-ridge interaction shapes the crustal thickness pattern of the Réunion hotspot track, *Geochem. Geophys. Geosyst.*, **18**(8), 2930–2948.

Bryan, S. E. & Ernst, R. E., 2008. Revised definition of Large Igneous Provinces (LIPs), *Earth-Science Reviews*, **86**(1), 175–202.

Bunge, H.-P., Richards, M. A., & Baumgardner, J. R., 2002. Mantle-circulation models with sequential data assimilation: inferring present-day mantle structure from plate-motion histories, *Phil. Trans. Roy. Soc. A*, **360**(1800), 2545–2567.

Burgess, S. D., Bowring, S. A., Fleming, T. H. & Elliot, D. H., 2015. High-precision geochronology links the Ferrar large igneous province with early-Jurassic ocean anoxia and biotic crisis, *Earth Planet. Sci. Lett.*, **415**, 90–99.

Burke, K., Steinberger, B., Torsvik, T. H., & Smethurst, M. A., 2008. Plume Generation Zones at the margins of Large Low Shear Velocity Provinces on the core-mantle boundary, *Earth Planet. Sci. Lett.*, **265**(1-2), 49–60.

Čížková, H., van den Berg, A., Spakman, W., & Matyska, C., 2012. The viscosity of Earth's lower mantle inferred from sinking speed of subducted lithosphere, *Phys. Earth Planet. Inter.*, **200–201**, 56–62.

Coffin, M. F., Pringle, M., Duncan, R., Gladczenko, T., Storey, M., Müller, R., & Gahagan, L., 2002. Kerguelen Hotspot Magma Output since 130 Ma, *Journal of Petrology*, **43**(7), 1121–1137.

Coffin, M. F., Duncan, R. A., Eldholm, O., Fitton, J. G., Frey, F. A., Larsen, H. C., Mahoney, J. J., Saunder, A. D., Schlich, R., & Wallace, P. J., 2006. Large igneous provinces and scientific ocean drilling: Status quo and a look ahead, *Oceanography*, **19**(4), 150–160.

Conrad, C. P. & Lithgow-Bertelloni, C., 2002. How mantle slabs drive plate tectonics, *Science*, **298**, 207–209.

Conrad, C. P., Steinberger, B., & Torsvik, T. H., 2013. Stability of active mantle upwelling revealed by net characteristics of plate tectonics, *Nature*, **498**, 479–482.

Cooper, A. F., Adam, L. J., Coulter, R. F., Eby, G. N. & McIntosh, W.C., 2007. Geology, geochronology and geochemistry of a basanitic volcano, White Island, Ross Sea, Antarctica, *Journal of Volcanology and Geothermal Research*, **165**, 189–216.

Courtillot, V., Davaille, A., Besse, J., & Stock, J., 2003. Three distinct types of hotspots in the Earth's mantle, *Earth Planet. Sci. Lett.*, **205**(3-4), 295–308.

Davies, G. F., 1977. Whole-mantle convection and plate tectonics, *Geophysical Journal of the Royal Astronomical Society*, **49**, 459–486.

Day, J. M. D., Harvey, R. P., & Hilton, D. R., 2019. Melt-modified lithosphere beneath Ross Island and its role in the tectono-magmatic evolution of the West Antarctic Rift System, *Chemical Geology*, **518**, 45–54.

de Vries, M. v. W., Bingham, R. G., & Hein, A. S., 2018. A new volcanic province: an inventory of subglacial volcanoes in West Antarctica, *Geological Society, London, Special Publications*, **461**(1), 231–248.

DeConto, R. M. & Pollard, D., 2003. Rapid Cenozoic glaciation of Antarctica induced by declining atmospheric CO_2., *Nature*, **421**, 245–249.

Domeier, M. & Torsvik, T. H., 2019. Full-plate modelling in pre-Jurassic time, *Geological Magazine*, **156**(2), 261–280.

Domeier, M., Doubrovine, P. V., Torsvik, T. H., Spakman, W., & Bull, A. L., 2016. Global correlation of lower mantle structure and past subduction, *Geophys. Res. Letters*, **43**, 4945–4953.

Doubrovine, P. V., Steinberger, B., & Torsvik, T. H., 2016. A failure to reject: Testing the correlation between large igneous provinces and deep mantle structures with EDF statistics, *Geochemistry, Geophysics, Geosystems*, **17**(3), 1130–1163.

Dziewonski, A. M. & Woodhouse, J. H., 1987. Global images of the Earth's interior, *Science*, **236**, 37–48.

Ebinger, C. J. & Sleep, N., 1998. Cenozoic magmatism throughout East Africa resulting from impact of a single plume, *Nature*, **395**(6704), 788–791.

Elliot, D. H. & Fleming, T. H., 2004. Occurrence and dispersal of magmas in the Jurassic Ferrar Large Igneous Province, Antarctica, *Gondwana Research*, **7**(1), 223–237.

Farnetani, D. G. & Richards, M. A., 1995. Thermal entrainment and melting in mantle plumes, *Earth*

Planet. Sci. Lett., **136**(3), 251 – 267.

Forsyth, D. & Uyeda, S., 1975. On the relative importance of the driving forces of plate motion, *Geophysical Journal of the Royal Astronomical Society*, **43**(1), 163–200.

Foulger, G. R., 2011. *Plates vs plumes: a geological controversy*, John Wiley & Sons.

Fox Maule, C., Purucker, M. E., Olsen, N., & Mosegaard, K., 2005. Heat flux anomalies in Antarctica revealed by satellite magnetic data, *Science*, **309**(5733), 464–467.

French, S. W. & Romanowicz, B., 2015. Broad plumes rooted at the base of the Earth's mantle beneath major hotspots, *Nature*, **525**, 95–99.

Fullea, J., Afonso, J. C., Connolly, J., Fernandez, M., García-Castellanos, D., & Zeyen, H., 2009. Litmod3d: An interactive 3-d software to model the thermal, compositional, density, seismological, and rheological structure of the lithosphere and sublithospheric upper mantle, *Geochemistry, Geophysics, Geosystems*, **10**(8).

Grand, S. P., 2002. Mantle shear–wave tomography and the fate of subducted slabs, *Philosophical Transactions of the Royal Society of London. Series A: Mathematical, Physical and Engineering Sciences*, **360**(1800), 2475–2491.

Griffiths, R. W. & Campbell, I. H., 1990. Stirring and structure in mantle starting plumes, *Earth Planet. Sci. Lett.*, **99**(1), 66 – 78.

Hager, B. H. & O'Connell, R. J., 1979. Kinematic models of large-scale flow in the Earth's mantle, *J. Geophys. Res.*, **84**, 1031–1048.

Hager, B. H. & O'Connell, R. J., 1981. A simple global model of plate dynamics and mantle convection, *J. Geophys. Res.*, **86**, 4843–4867.

Hager, B. H. & Richards, M. A., 1989. Long-wavelength variations in Earth's geoid: physical models and dynamical implications, *Phil. Trans. R. Soc. London Ser. A*, **328**, 309–327.

Hansen, S. E., Graw, J. H., Kenyon, L. M., Nyblade, A. A., Wiens, D. A., Aster, R. C., Huerta, A. D., Anandakrishnan, S., & Wilson, T., 2014. Imaging the Antarctic mantle using adaptively parameterized p-wave tomography: Evidence for heterogeneous structure beneath West Antarctica, *Earth and Planetary Science Letters*, **408**, 66 – 78.

Heister, T., Dannberg, J., Gassmöller, R., & Bangerth, W., 2017. High accuracy mantle convection simulation through modern numerical methods. II: Realistic models and problems, *Geophysical Journal International*, **210**(2), 833–851.

Hoggard, M. J., White, N., & Al-Attar, D., 2016. Global dynamic topography observations reveal limited influence of large-scale mantle flow, *Nat. Geosci.*, **9**, 456–463.

Hole, M. J., & LeMasurier, W. E., 1994. Tectonic controls on the geochemical composition of Cenozoic, mafic alkaline volcanic rocks from West Antarctica, *Contributions to Mineralogy and Petrology*, bf 117, 187–202.

Hosseini, K., Sigloch, K., Tsekhmistrenko, M., Zaheri, A., Nissen-Meyer, T., & Igel, H., 2019. Global mantle structure from multi-frequency tomography using p, pp and p-diffracted waves, *Geophysical Journal International*.

Justo, J., Morra, G., & Yuen, D., 2015. Viscosity undulations in the lower mantle: The dynamical role of iron spin transition, *Earth and Planetary Science Letters*, **421**, 20 – 26.

King, S. D., 2007. Hotspots and edge-driven convection, *Geology*, **35**(3), 223.

King, S. D., 2016. An evolving view of transition zone and midmantle viscosity, *Geochemistry, Geophysics, Geosystems*, **17**(3), 1234–1237.

King, S. D. & Adam, C., 2014. Hotspot swells revisited, *Physics of the Earth and Planetary Interiors*, **235**, 66 – 83.

Korenaga, J., 2008. Urey ratio and the structure and evolution of Earth's mantle, *Reviews of Geophysics*, **46**, RG2007.

Korenaga, J., 2016. Can mantle convection be self-regulated?, *Science Advances*, **235**, 66–83.

Kronbichler, M., Heister, T., & Bangerth, W., 2012. High accuracy mantle convection simulation through modern numerical methods, *Geophysical Journal International*, **191**, 12–29.

Kyle, P., Moore, J., & Thirlwall, M., 1992. Petrologic evolution of anorthoclase phonolite lavas at Mount Erebus, Ross Island, Antarctica, *Journal of Petrology*, **33**(4), 849–875.

Larter, R. D., Cunningham, A. P., Barker, P. F., Gohl, K., & Nitsche, F. O., 2002. Tectonic evolution of the Pacific margin of Antarctica 1. Late Cretaceous tectonic reconstructions, *Journal of Geophysical Research: Solid Earth*, **107**(B12), EPM–5.

Lau, H., Mitrovica, J., Austermann, J., Crawford, O., Al-Attar, D., & Latychev, K., 2016. Inferences of mantle viscosity based on ice age data sets: Radial structure, *J. Geophys. Res. Solid Earth*, **121**, 6991–7012.

LeMasurier, W., 2013. Shield volcanoes of Marie Byrd Land, West Antarctic Rift: oceanic island similarities, continental signature, and tectonic controls, *Bulletin of volcanology*, **75**(6), 726.

LeMasurier, W. & Rex, D., 1989. Evolution of linear volcanic ranges in Marie Byrd Land, West Antarctica, *Journal of Geophysical Research: Solid Earth*, **94**(B6), 7223–7236.

Liu, X. & Zhong, S., 2016. Constraining mantle viscosity structure for a thermochemical mantle using the geoid observation, *Geochemistry, Geophysics, Geosystems*, **17**(3), 895–913.

Lloyd, A. J., 2018. Seismic tomography of Antarctica and the southern oceans: Regional and continental models from the upper mantle to the transition zone, *PhD Thesis, Washington University in St. Louis*.

Lloyd, A. J., Wiens, D. A., Nyblade, A. A., Anandakrishnan, S., Aster, R. C., Huerta, A. D., Wilson, T. J., Dalziel, I. W. D., Shore, P. J., & Zhao, D., 2015. A seismic transect across West Antarctica: Evidence for mantle thermal anomalies beneath the Bentley Subglacial Trench and the Marie Byrd

Land Dome, *Journal of Geophysical Research: Solid Earth*, **120**(12), 8439–8460.

Marquardt, H. & Miyagi, L., 2015. Slab stagnation in the shallow lower mantle linked to an increase in mantle viscosity, *Nature Geosci.*, **8**, 311–314.

Martin, A. P., Cooper, A. F. & Price, R. C., 2013. Petrogenesis of Cenozoic, alkalic volcanic lineages at Mount Morning, West Antarctica and their entrained lithospheric mantle xenoliths: Lithospheric versus asthenospheric mantle sources, *Geochimica et Cosmochimica Acta*, **122**, 127–152.

Martos, Y. M., Catalán, M., Jordan, T. A., Golynsky, A., Golynsky, D., Eagles, G., & Vaughan, D. G., 2017. Heat flux distribution of Antarctica unveiled, *Geophysical Research Letters*, **44**(22), 11,417–11,426.

Mazzullo, A., Stutzmann, E., Montagner, J.-P., Kiselev, S., Maurya, S., Barruol, G., & Sigloch, K., 2017. Anisotropic tomography around Réunion island from Rayleigh waves, *J. Geophys. Res. Solid Earth*, **122**.

Montelli, R., Nolet, G., Dahlen, F., & Masters, G., 2006. A catalogue of deep mantle plumes: New results from finite-frequency tomography, *Geochemistry, Geophysics, Geosystems*, **7**(11).

Moreira, M. & Allègre, C. J., 1998. Helium–neon systematics and the structure of the mantle, *Chemical Geology*, **147**(1), 53 – 59.

Morgan, W. J., 1971. Convection plumes in the lower mantle, *Nature*, **230**, 42–43.

Morgan, W. J., 1972. Deep mantle convection plumes and plate motions, *AAPG bulletin*, **56**(2), 203–213.

Nakada, M., Okuno, J., & Irie, Y., 2017. Inference of viscosity jump at 670 km depth and lower mantle viscosity structure from GIA observations, *Geophysical Journal International*, **212**(3), 2206–2225.

Nardini, I., Armienti, P., Rocchi, S., Dallai, L., Harrison, D., 2009. Sr–Nd–Pb–He–O Isotope and Geochemical Constraints on the Genesis of Cenozoic Magmas from the West Antarctic Rift, *Journal of Petrology*, **50**(7), 1359–1375.

Panter, K. S., Kyle, P. R., & Smellie, J. L., 1997. Petrogenesis of a phonolite–trachyte succession at Mount Sidley, Marie Byrd Land, Antarctica, *Journal of Petrology*, **38**(9), 1225–1253.

Panter, K. S., Hart, S. R., Kyle, P., Blusztanjn, J., & Wilch, T., 2000. Geochemistry of late Cenozoic basalts from the Crary Mountains: characterization of mantle sources in Marie Byrd Land, Antarctica, *Chemical Geology*, **165**(3-4), 215–241.

Panter, K. S., Castillo, P., Krans, S., Deering, C., McIntosh, W., Valley, J. W., Kitajima, K., Kyle, P., Hart, S., Blusztajn, J., 2018. Melt origin across a rifted continental margin: a case for subduction-related metasomatic agents in the lithospheric source of alkaline basalt, northwest Ross Sea, Antarctica. *Journal of Petrology*, **59**, 517–558.

Pappa, F., Ebbing, J., Ferraccioli, F., & van der Wal, W., 2019. Modeling satellite gravity gradient data to derive density, temperature, and viscosity structure of the Antarctic lithosphere, *Journal of*

Geophysical Research: Solid Earth, **124**(11), 12053–12076.

Paxman, G., Jamieson, S., Hochmuth, K., Gohl, K., Bentley, M., Leitchenkov, G., & Ferraccioli, F., 2019. Reconstructions of Antarctic topography since the Eocene–Oligocene boundary, *Palaeogeography, Palaeoclimatology, Palaeoecology*, **535**, 109346.

Phillips, E. H., Sims, K. W., Blichert-Toft, J., Aster, R. C., Gaetani, G. A., Kyle, P. R., Wallace, P. J., & Rasmussen, D. J., 2018. The nature and evolution of mantle upwelling at Ross Island, Antarctica, with implications for the source of HIMU lavas, *Earth and Planetary Science Letters*, **498**, 38–53.

Putirka, K., 2008. Excess temperatures at ocean islands: Implications for mantle layering and convection, *Geology*, **36**(4), 283–286.

Ricard, Y., Richards, M., Lithgow-Bertelloni, C., & Le Stunff, Y., 1993. A geodynamic model of mantle density heterogeneity, *Journal of Geophysical Research: Solid Earth*, **98**(B12), 21895–21909.

Richards, M. A. & Engebretson, D. C., 1992. Large-scale mantle convection and the history of subduction, *Nature*, **355**, 437–330.

Richards, M. A., Duncan, R. A., & Courtillot, V. E., 1989. Flood Basalts and Hot-Spot Tracks: Plume Heads and Tails, *Science*, **246**, 103–107.

Rocchi S., Storti F., Di Vincenzo G., & Rosetti F., 2003. Intraplate strike-slip tectonics as an alternative to mantle plume activity for the Cenozoic rift magmatism in the Ross Sea region, Antarctica. In Intraplate Strike-Slip Deformation Belts (eds. F. Storti, R. E. Holdsworth and F. Salvini). Special Publication, Geological Society London, pp. 145–158.

Rocchi S., Armienti P., & Di Vincenzo G., 2005. No plume, no rift magmatism in the West Antarctic Rift. In Plates, Plumes and Paradigms (eds. G. R. Foulger, J. H. Natland, D. C. Presnall and D. L. Anderson). Geological Society of America Special Paper, pp. 435-447.

Rocholl, A., Stein, M., Molzahn, M., Hart, S., & Wörner, G., 1995. Geochemical evolution of rift magmas by progressive tapping of a stratified mantle source beneath the Ross Sea Rift, Northern Victoria Land, Antarctica, *Earth and Planetary Science Letters*, **131**(3), 207 – 224.

Roy, K. & Peltier, W., 2015. Glacial isostatic adjustment, relative sea level history and mantle viscosity: reconciling relative sea level model predictions for the us east coast with geological constraints., *Geophys. J. Int.*, **201**, 1156–1181.

Rudolph, M. L., Lekić, V., & Lithgow-Bertelloni, C., 2015. Viscosity jump in Earth's mid-mantle, *Science*, **350**, 1349–1352.

Schaeffer, A. & Lebedev, S., 2013. Global shear speed structure of the upper mantle and transition zone, *Geophysical Journal International*, **194**, 417–449.

Schilling, J.-G., 1991. Fluxes and excess temperatures of mantle plumes inferred from their interaction with migrating mid-ocean ridges, *Nature*, **352**, 397–403.

Schubert, G., Turcotte, D. L., & Olson, P., 2001. *Mantle convection in the Earth and planets*, Cambridge Univ. Press, Cambridge, U. K.

Seroussi, H., Ivins, E. R., Wiens, D. A., & Bondzio, J., 2017. Influence of a West Antarctic mantle plume on ice sheet basal conditions, *Journal of Geophysical Research: Solid Earth*, **122**(9), 7127–7155.

Shapiro, N. M. & Ritzwoller, M. H., 2004. Inferring surface heat flux distributions guided by a global seismic model: particular application to Antarctica, *Earth and Planetary Science Letters*, **223**(1), 213 – 224.

Shen, W., Wiens, D. A., Anandakrishnan, S., Aster, R. C., Gerstoft, P., Bromirski, P. D., Hansen, S. E., Dalziel, I. W., Heeszel, D. S., Huerta, A. D., et al., 2018. The crust and upper mantle structure of Central and West Antarctica from Bayesian inversion of Rayleigh wave and receiver functions, *Journal of Geophysical Research: Solid Earth*, **123**(9), 7824–7849.

Shephard, G., Bunge, H.-P., Schuberth, B., Müller, R., Talsma, A., Moder, C., & Landgrebe, T., 2012. Testing absolute plate reference frames and the implications for the generation of geodynamic mantle heterogeneity structure, *Earth and Planetary Science Letters*, **317**-**318**, 204 – 217.

Sleep, N. H., 1997. Lateral flow and ponding of starting plume material, *J. Geophys. Res.*, **102**(B5), 10001–10012.

Sleep, N. H., 2006. Mantle plumes from top to bottom, *Earth-Science Reviews*, **77**(4), 231 – 271.

Sleep, N. H., 2007. Edge-modulated stagnant-lid convection and volcanic passive margins, *Geochemistry, Geophysics, Geosystems*, **8**(12).

Steinberger, B., 2000. Plumes in a convecting mantle: Models and observations for individual hotspots, *J. Geophys. Res.*, **105**(B5), 11,127–11,152.

Steinberger, B. & Calderwood, A., 2006. Models of large-scale viscous flow in the Earth's mantle with constraints from mineral physics and surface observations, *Geophys. J. Int.*, **167**, 1461–1481.

Steinberger, B. & O'Connell, R. J., 1998. Advection of plumes in mantle flow: implications for hotspot motion, mantle viscosity and plume distribution, *Geophysical Journal International*, **132**(2), 412–434.

Steinberger, B., Torsvik, T. H., & Becker, T. W., 2012. Subduction to the lower mantle - a comparison between geodynamic and tomographic models, *Solid Earth*, **3**, 415–432.

Steinberger, B., Conrad, C., Osei Tutu, A., & Hoggard, M., 2019a. On the amplitude of dynamic topography at spherical harmonic degree two, *Tectonophysics*, **760**, 221–228.

Steinberger, B., Nelson, P., Grand, S., & Wang, W., 2019b. Yellowstone plume conduit tilt caused by large-scale mantle flow, *Geochemistry, Geophysics, Geosystems*.

Torsvik, Trond H. Svensen, H. H., Steinberger, B., Royer, D. L., Jerram, D. A., Jones, M. T., & Domeier, M., 2020. Connecting the deep Earth and the atmosphere, in *Mantle convection and surface expression*, Geophys. Monograph, eds Cottaar, S., Marquardt, H., Konter, J., & Ballmer, M., American Geophysical Union, Washington, DC.

Torsvik, T. H., Smethurst, M. A., Burke, K., & Steinberger, B., 2006. Large igneous provinces generated from the margins of the large low-velocity provinces in the deep mantle, *Geophys. J. Int.*, **167**(3), 1447–1460.

Torsvik, T. H., Steinberger, B., Gurnis, M., & Gaina, C., 2010. Plate tectonics and net lithosphere rotation over the past 150 My, *Earth Planet. Sci. Lett.*, **291**(1-4), 106–112.

Tozer, D. C., 1972. The present thermal state of the terrestrial planets, *Phys. Earth Planet. Inter.*, **6**(1-3), 182–197.

van der Meer, D. G., Spakman, W., van Hinsbergen, D. J. J., Amaru, M. L., & Torsvik, T. H., 2010. Towards absolute plate motions constrained by lower-mantle slab remnants, *Nature Geoscience*, **3**, 36–40.

van Keken, P., 1997. Evolution of starting mantle plumes: a comparison between numerical and laboratory models, *Earth Planet. Sci. Lett.*, **148**(1), 1 – 11.

van Wijk, J., Lawrence, J., & Driscoll, N., 2008. Formation of the Transantarctic Mountains related to extension of the West Antarctic Rift System, *Tectonophysics*, **458**(1-4), 117–126.

Whitehead, J. A. & Luther, D. S., 1975. Dynamics of laboratory diapir and plume models, *Journal of Geophysical Research*, **80**(5), 705–717.

Wilson, J. T., 1963. A possible origin of the Hawaiian Islands, *Canadian Journal of Physics*, **41**(6), 863–870.

Yang, T. & Gurnis, M., 2016. Dynamic topography, gravity and the role of lateral viscosity variations from inversion of global mantle flow, *Geophysical Journal International*, **207**(2), 1186–1202.